

Classification of Awareness in Disorders of Consciousness Using Common Spatial Pattern

Chaewon Lee¹, Sunho Lee², Jitka Annen^{3,4}, Ji-Hoon Jeong⁵, Marcello Massimini⁶,
Silvia Casarotto⁶, Melanie Boly⁷, Olivier Bodart³, Aurore Thibaut³,
Mario Rosanova⁶, Steven Laureys^{8,9}, Olivia Gosseries^{3,8,9*}, and Minji Lee^{2*}

¹Dept. Data Science, The Catholic University of Korea, Bucheon, Republic of Korea

²Dept. Biomedical Software Engineering, The Catholic University of Korea, Bucheon, Republic of Korea

³Dept. GIGA-Research & Neurology, University and University Hospital of Liege, Liege, Belgium

⁴Dept. Data Analysis, University of Ghent, B9000, Ghent, Belgium

⁵Dept. Computer Science, Chungbuk National University, Cheongju, Republic of Korea

⁶Dept. Biomedical and Clinical Sciences “L. Sacco”, University of Milan, Milan, Italy

⁷Wisconsin Institute for Sleep and Consciousness, Dept. Psychiatry, University of Wisconsin, Madison, USA

⁸Coma Science Group, GIGA-Consciousness, GIGA Research Center, University of Liège, Liège, Belgium

⁹Centre du Cerveau, Neurology department, University Hospital of Liège, Liège, Belgium

Email: ogosseries@uliege.be, minjilee@catholic.ac.kr (* Corresponding authors)

Abstract—Advances in intensive care have improved the survival rate of patients with severe acute brain injury, but diagnostic errors for patients with disorders of consciousness are still high. Accurate diagnosis of these patients is very important because effective treatment can vary depending on the diagnosis. In this study, we propose a framework for classifying unresponsive wakefulness syndrome and minimally conscious state, focusing on awareness. In particular, power spectral density and common spatial patterns were used together, considering that spatial information is a key feature in consciousness. The 16 patients with unresponsive wakefulness syndrome and 14 with minimally conscious state underwent resting-state electroencephalography measurements. In addition, we compared the performance by utilizing each frequency (delta, theta, alpha, beta, gamma bands) related to consciousness. As a result, the highest accuracy of 95.06% was achieved by the EEGNet classifier, especially in the beta frequency band. We demonstrated that spatial information is very important in consciousness, as we observed that classifica-

tion performance improved when common spatial patterns were used. These results provide insight into various frameworks for diagnosing patients with disorders of consciousness and may help patients survive by increasing the diagnosis rate in the future.

Index Terms—disorders of consciousness, electroencephalography, common spatial pattern, classification

I. INTRODUCTION

Disorders of consciousness (DoC) is a group of altered consciousness states generally caused by injury dysfunction of the neural systems regulating arousal and awareness. When patients fall into a coma after brain injury, they show an absence of both arousal (i.e., eye opening even when stimulated) and awareness (i.e., unaware of themselves and the environment) [1]. Unresponsive wakefulness syndrome (UWS), also known as the vegetative state [2], refers to a state where a patient is awake but lacks awareness [3]. Minimally conscious state (MCS), on the other hand, describes a condition where patients recover to a transient or chronic state of reduced responsiveness, but still show intermittent and limited signs of awareness of themselves and their surroundings [3]. In this regard, when treating DoC patients, making an accurate diagnosis early on is crucial for developing personalized treatment plans. Therefore, neuroimaging-assisted diagnosis are needed for more accurate and rapid diagnosis of DoC patients.

Resting-state electroencephalography (EEG) is closely related to the brain’s baseline activity and can help monitor a patient’s level of consciousness. EEG signals are divided into several frequency bands. Delta band, characterized by high amplitude and slow frequency, is associated with deep sleep [4]. In DoC patients, an increase in delta power as observed with resting-state EEG may indicate severe consciousness impairment, resembling patterns observed in deep

This work was partly supported by the IITP (Institute of Information & Communications Technology Planning & Evaluation)-ICAN (ICT Challenge and Advanced Network of HRD)(IITP-2024-RS-2024-00438207, 50%) grant funded by the Korea government (Ministry of Science and ICT) and National Research Foundation of Korea (NRF) grant funded by the Korea government(MSIT) (No. RS-2024-00336880). The study was further supported by the University and University Hospital of Liège, the Belgian National Funds for Scientific Research (FRS-FNRS), the FNRS PDR project (T.0134.21), the FNRS MIS project (F.4521.23), the FLAG-ERA JTC2021 project ModelDXConsciousness (Human Brain Project Partnering Project) and FLAG-ERA JTC 2023 - HBP - Basic and Applied Research, project BrainAct, the fund Generet, the King Baudouin Foundation, the Funds Chantal Schaeck Yolande, the BIAL Foundation, the Mind Science Foundation, the European Commission, the Fondation Leon Fredericq, the Mind-Care foundation, the Horizon 2020 MSCA – Research and Innovation Staff Exchange DoC-Box project (HORIZON-MSCA-2022-SE-01-01; 101131344). OG & AT are Research Associates and SL research director at FRS-FNRS. JA is postdoctoral fellow funded (1265522N) by the Fund for Scientific Research-Flanders (FWO). (* Corresponding authors)

sleep. Another important frequency band is theta band, which is associated with memory, attention, and cognitive processing [5]. The alpha band is also crucial, as it is related to the brain's resting state when the eyes are closed [6] and has been linked to DoC in previous studies [7]. The beta band is commonly linked to active cognitive functions, such as thinking, problem-solving, and arousal [8]. On the other hand, the gamma band is associated with functions like information binding, sensory integration, and conscious perception [9]. The presence of gamma oscillations, especially in the parietal and frontal regions, can suggest the potential for higher-order cognitive processing and awareness [10]. In this regard, using resting-state EEG in DoC patients allows for a better assessment of the severity of brain damage, providing insights into the prognosis and the processes underlying different states of consciousness [1].

Many researchers have proposed methods to distinguish between UWS and MCS patients using resting-state EEG signals. Raveendran et al. [11] utilized the variational mode decomposition (VMD) for feature extraction to perform binary classification between UWS and MCS. They achieved a classification accuracy of 83.3% using the ensemble boosting trees model. However, the VMD method has limitations in that the analysis time is considerably long and the performance is still low. In addition, there are various studies that classify DoC patients by adding coma [1], [4] or healthy controls [12]. However, coma is more distinct than UWS and MCS in that both awareness and arousal are absent. It is rather because there is no arousal, no eye opening whatsoever and thus it is easy at the clinical level to differentiate from UWS/MCS who both have arousal - i.e., eye open. So the classification of these two seems more difficult. In this respect, MCS is also subdivided into MCS+ and MCS- depending on the presence. Chennu et al. [2] quantified the spectral connectivity estimated from EEG signals and performed a three-class classification between UWS, MCS+, and MCS-. Using a support vector machine, they achieved an area under the curve (AUC) of 0.77 and 0.78 in non-traumatic and traumatic aetiologies, respectively.

Conventional EEG discrimination approaches often relied on calculating power spectral density (PSD) at each electrode and mapping these values for visualization. However, these methods could produce errors by treating processes at different electrode sites as independent and overlooking the spatial correlation in EEG signals. There is a key area in consciousness called the posterior hot zone, which shows prominent changes depending on the state of consciousness [13]. In this respect, spatial information can also be used as a very important feature in the classification of DoC patients. Common spatial pattern (CSP) is used to maximize the discriminative power by enhancing the differences between the EEG data of two groups, and is actually an important feature commonly used in brain-computer interfaces [14]. It provides information about spatial differences by extracting CSP from the EEG of each group, optimizing the variance of one group, and minimizing the variance of the other group. Therefore, CSP addresses

this limitation by calculating spatial covariance to optimize classification between groups [15].

In this study, we propose a framework to classify UWS and MCS using resting-state EEG signals. In particular, considering the importance of spatial information in consciousness, we combined CSP with PSD and utilized it as a feature. Therefore, we hypothesized that the classification performance would be improved when it was used with CSP with PSD, compared to when PSD was used as a feature alone. Additionally, we compared the performance of five frequency bands (delta, theta, alpha, beta, and gamma bands) as features to find the frequency band most closely associated with awareness in distinguishing UWS and MCS. Finally, K-nearest neighbors (KNN), random forest (RF), gradient boosting (GB), and EEG-Net [16] are used as classifiers in this study. This framework contributes to reducing diagnostic errors in DoC patients by providing clues to the frequency bands and features most important for distinguishing UWS and MCS for awareness, a key element of consciousness.

II. METHODS

A. Dataset

The dataset consisted of 16 UWS patients (8 males, mean age 40.19 ± 23.99 years, mean time since injury 9.94 ± 12.86 months) and 14 MCS patients (9 males, mean age 40.36 ± 18.82 years, mean time since injury 52.64 ± 90.17 months). The dataset used in this study was previously published in Bodart et al. [17], [18], Rosanova et al. [19], and Lee et al. [20]. This study was approved by the Ethics Committee of the Medicine Faculty of the University of Liège (ref 2009/52) and written informed consent was obtained from legal representatives of all patients.

EEG signals were measured during a resting state with eyes closed for 5 min using a 60-channel EEG system. The sampling rate was 1,450 Hz. The signals were downsampled to 362.5 Hz and then underwent bandpass filtering using a second-order Butterworth filter within 0.5–45 Hz. Channels with poor quality were manually identified and interpolated using high-order spherical interpolation for artifact removal. The continuous signal was segmented into 2-sec intervals. Additionally, independent component analysis was applied to eliminate components associated with eye movements, and a threshold of $\pm 100 \mu V$ was set to exclude trials affected by eye artifacts and other noise. After preprocessing, the data were re-referenced using an average reference method.

B. Feature Extraction

We applied second-order Butterworth bandpass filtering to separate the frequency bands into delta (1.5–4 Hz), theta (4–8 Hz), alpha (8–13 Hz), beta (13–30 Hz), and gamma (30–40 Hz) [20].

1) *Power Spectral Density*: This is a measure that describes how the power of a signal or time series is distributed across different frequency components. PSD improves classification

accuracy by calculating power density across various frequencies, making the differences between classification targets more distinct [21].

We employed the Welch method, which is expressed as follows:

$$P_{xx}(f) = \frac{1}{N} \sum_{k=1}^N P_{xx,k}(f) \quad (1)$$

where N represents the number of data segments used for calculating the PSD, while k serves as the index for each individual trial or segment. This approach involves segmenting the signal into overlapping sections, computing the spectrum for each section individually, and then averaging these spectra to obtain the final estimate [22].

2) *Common Spatial Pattern* : This is primarily applied in binary classification, aiming to find spatial filters that minimize the variance within one class while maximizing the variance between classes [15].

$$Q(a) = \frac{a^T P_2^T P_2 a}{a^T P_1^T P_1 a} = \frac{a^T C_2 a}{a^T C_1 a} \quad (2)$$

where T denotes the transpose of a matrix, while P_i represents the training data matrix, organized with sample points as rows and channels as columns. The spatial covariance matrix for a specific class i is denoted as C_i . To solve the optimization problem, we employ the method of Lagrange multipliers to minimize the following function [23]:

$$L(\gamma, a) = a^T C_1 a - \gamma(a^T C_2 a - 1) \quad (3)$$

When the derivative of L with respect to a is zero, γ represents the Lagrange multiplier, and the filter a that minimizes L satisfies the following relationship [23]:

$$\frac{\partial L}{\partial a} = 2a^T C_1 - 2\gamma a^T C_2 = 0 \leftrightarrow C_1 a = \gamma C_2 a \quad (4)$$

This transforms into a standard eigenvalue problem. Consequently, the spatial filters that minimize the function (2) are obtained using the eigenvectors of $Z = C_2^{-1} C_1$. These filters encompass two components corresponding to the largest and smallest eigenvalues. These are extracted as the logarithm of the variance of the EEG signals in the selected band after projecting the filter a onto the CSP matrix [23].

C. Classification

We used four classifiers as follows: KNN, RF, GB, and EEGNet [16]. KNN, while a relatively simple algorithm, demonstrated excellent performance on small datasets and was chosen due to its suitability for binary classification tasks [24]. RF, an ensemble model composed of multiple decision trees, is effective in reducing overfitting and improving generalization. Additionally, GB, which incrementally trains weak classifiers to enhance performance, was selected for its potential to achieve high accuracy [25]. EEGNet, a deep learning architecture specifically designed for processing EEG data, utilizes convolutional layers to extract spatial features and is known for its efficiency and effectiveness in classifying brain activity [16].

TABLE I
HYPERPARAMETER FOR EACH MODEL

| Model | Hyperparameter |
|--------|--|
| KNN | n_neighbors=5, p=1 |
| RF | n_estimators=50, max_features='sqrt' |
| GB | n_estimators=100, learning_rate=0.1 |
| EEGNet | Batch size=32, Epoch=100 Learning rate=0.001 Optimizer=RMSprop, Dropout rate=0.3 |

We used the 10-fold cross-validation for model evaluation [11]. This method enhances the reliability of performance evaluation by accurately reflecting the characteristics of the dataset [26]. Hyperparameter tuning was conducted to optimize the performance of each model, and the key hyperparameters used are presented in Table I.

D. Evaluation Metrics

In this study, we utilized accuracy, precision, and F1-score as the primary evaluation metrics to assess the classification performance of the models. Accuracy represents the proportion of correctly predicted samples among all samples [27].

$$\text{Accuracy} = \frac{TP + TN}{TP + TN + FP + FN} \quad (5)$$

where TP denotes true positive, TN denotes true negative, FP denotes false positive, and FN denotes false negative. Precision, on the other hand, indicates the proportion of actual positive samples among those predicted as positive, defined as [28]:

$$\text{Precision} = \frac{TP}{TP + FP} \quad (6)$$

Recall, also known as sensitivity, measures the proportion of actual positive samples that were correctly identified as [28]:

$$\text{Recall} = \frac{TP}{TP + FN} \quad (7)$$

Additionally, F1-score is the harmonic mean of precision and recall, making it a useful metric for evaluating model performance in the context of imbalanced datasets. The F1-score is defined as [28]:

$$\text{F1-score} = 2 \times \frac{\text{precision} \times \text{recall}}{\text{precision} + \text{recall}} \quad (8)$$

Through these evaluation metrics, the predictive performance of the models was assessed from multiple perspectives.

E. Statistical Analysis

Statistical analysis was used to compare the performances of different features and classifiers. First, the t -test was used to compare the performance using PSD and the performance using PSD and CSP simultaneously. Next, when comparing performances from four models and performances across five frequency bands, a one-way analysis of variance was used to check whether the differences in performances were statistically significant. Then t -test was used as a post hoc test using

TABLE II
CLASSIFICATION PERFORMANCE FOR CLASSIFYING UWS AND MCS IN DOC PATIENTS

| Feature | Model | Frequency band | Accuracy (%) | Precision | Recall | F1-Score |
|---------|--------|----------------|--------------------------------------|-------------------------------------|-------------------------------------|-------------------------------------|
| PSD | KNN | Delta | 69.88 (± 3.11) | 0.68 (± 0.04) | 0.66 (± 0.03) | 0.67 (± 0.03) |
| | | Theta | 70.24 (± 2.85) | 0.68 (± 0.03) | 0.69 (± 0.05) | 0.68 (± 0.02) |
| | | Alpha | 73.22 (± 3.12) | 0.73 (± 0.05) | 0.67 (± 0.03) | 0.70 (± 0.03) |
| | | Beta | 93.97 (± 1.35) | 0.93 (± 0.02) | 0.93 (± 0.02) | 0.93 (± 0.01) |
| | | Gamma | 87.14 (± 1.97) | 0.87 (± 0.03) | 0.85 (± 0.02) | 0.86 (± 0.01) |
| | RF | Delta | 69.49 (± 3.06) | 0.67 (± 0.02) | 0.65 (± 0.05) | 0.66 (± 0.03) |
| | | Theta | 70.94 (± 2.89) | 0.70 (± 0.04) | 0.66 (± 0.04) | 0.67 (± 0.02) |
| | | Alpha | 75.76 (± 2.85) | 0.75 (± 0.04) | 0.70 (± 0.04) | 0.73 (± 0.03) |
| | | Beta | 92.98 (± 1.69) | 0.92 (± 0.02) | 0.92 (± 0.02) | 0.92 (± 0.01) |
| | | Gamma | 86.71 (± 1.98) | 0.86 (± 0.03) | 0.85 (± 0.02) | 0.85 (± 0.02) |
| | GB | Delta | 71.80 (± 4.34) | 0.71 (± 0.05) | 0.67 (± 0.04) | 0.69 (± 0.04) |
| | | Theta | 72.04 (± 4.34) | 0.72 (± 0.05) | 0.64 (± 0.05) | 0.68 (± 0.03) |
| | | Alpha | 76.35 (± 2.78) | 0.75 (± 0.04) | 0.72 (± 0.03) | 0.74 (± 0.03) |
| | | Beta | 93.33 (± 1.22) | 0.92 (± 0.01) | 0.93 (± 0.02) | 0.92 (± 0.01) |
| | | Gamma | 85.53 (± 2.03) | 0.83 (± 0.03) | 0.85 (± 0.02) | 0.84 (± 0.01) |
| | EEGNet | Delta | 73.73 (± 0.03) | 0.73 (± 0.04) | 0.68 (± 0.06) | 0.70 (± 0.03) |
| | | Theta | 74.55 (± 0.03) | 0.74 (± 0.04) | 0.69 (± 0.04) | 0.71 (± 0.03) |
| | | Alpha | 79.49 (± 0.02) | 0.79 (± 0.03) | 0.75 (± 0.04) | 0.77 (± 0.03) |
| | | Beta | 94.39 (± 0.01) | 0.93 (± 0.02) | 0.94 (± 0.02) | 0.94 (± 0.01) |
| | | Gamma | 86.43 (± 0.02) | 0.87 (± 0.03) | 0.82 (± 0.03) | 0.85 (± 0.02) |
| PSD+CSP | KNN | Delta | 77.81 (± 2.42) | 0.75 (± 0.02) | 0.77 (± 0.02) | 0.76 (± 0.01) |
| | | Theta | 81.18 (± 2.52) | 0.80 (± 0.02) | 0.80 (± 0.03) | 0.80 (± 0.02) |
| | | Alpha | 83.61 (± 3.02) | 0.82 (± 0.03) | 0.78 (± 0.03) | 0.80 (± 0.02) |
| | | Beta | 93.45 (± 1.46) | 0.93 (± 0.02) | 0.95 (± 0.01) | 0.94 (± 0.01) |
| | | Gamma | 91.65 (± 1.16) | 0.91 (± 0.02) | 0.90 (± 0.01) | 0.91 (± 0.01) |
| | RF | Delta | 76.04 (± 3.45) | 0.75 (± 0.05) | 0.72 (± 0.04) | 0.73 (± 0.03) |
| | | Theta | 83.07 (± 2.68) | 0.83 (± 0.02) | 0.80 (± 0.03) | 0.81 (± 0.02) |
| | | Alpha | 85.02 (± 2.65) | 0.84 (± 0.05) | 0.83 (± 0.03) | 0.83 (± 0.03) |
| | | Beta | 93.61 (± 1.16) | 0.93 (± 0.02) | 0.93 (± 0.02) | 0.93 (± 0.01) |
| | | Gamma | 91.57 (± 1.75) | 0.93 (± 0.02) | 0.88 (± 0.03) | 0.90 (± 0.01) |
| | GB | Delta | 79.73 (± 3.43) | 0.79 (± 0.04) | 0.75 (± 0.03) | 0.77 (± 0.03) |
| | | Theta | 84.27 (± 1.94) | 0.83 (± 0.01) | 0.82 (± 0.03) | 0.82 (± 0.02) |
| | | Alpha | 85.96 (± 2.26) | 0.84 (± 0.04) | 0.84 (± 0.02) | 0.84 (± 0.02) |
| | | Beta | 93.86 (± 1.55) | 0.92 (± 0.02) | 0.92 (± 0.02) | 0.92 (± 0.01) |
| | | Gamma | 90.86 (± 1.98) | 0.90 (± 0.02) | 0.89 (± 0.03) | 0.90 (± 0.02) |
| | EEGNet | Delta | 75.22 (± 0.03) | 0.72 (± 0.04) | 0.75 (± 0.06) | 0.73 (± 0.03) |
| | | Theta | 80.51 (± 0.03) | 0.78 (± 0.05) | 0.79 (± 0.04) | 0.79 (± 0.03) |
| | | Alpha | 88.98 (± 0.01) | 0.87 (± 0.02) | 0.88 (± 0.02) | 0.88 (± 0.01) |
| | | Beta | 95.06 (± 0.01) | 0.94 (± 0.02) | 0.94 (± 0.02) | 0.94 (± 0.01) |
| | | Gamma | 91.41 (± 0.02) | 0.91 (± 0.02) | 0.90 (± 0.03) | 0.90 (± 0.02) |

Mean (\pm standard deviation); bold = the highest performance in each metric.

false discovery rate (FDR) correction. The p -value was calculated to assess the statistical significance of the findings, with a p -value less than 0.05 indicating a statistically significant difference with FDR correction for multiple comparisons.

III. RESULTS AND DISCUSSION

A. Classification Performance

Table II shows the classification performance for distinguishing between UWS and MCS, and the highest performance is achieved with 95.06% accuracy, which utilizes both CSP and PSD in the beta band and uses EEGNet.

1) *Feature*: When comparing the performance of using only PSD and the performance of using PSD and CSP together in four models and five frequency bands, the performance of using PSD and CSP together was statistically significantly higher in most cases. Detailed statistical values are shown in Table III. Only in the case of using the delta band in EEGNet,

there was no statistical difference between using only PSD and using both PSD and CSP. In addition, there is not much difference in performance when CSP is used together with the beta band.

The relatively small performance differences between the models in the PSD-only scenario suggest that CSP helps to clarify these differences. This implies that CSP enhances the information provided by PSD and helps the models learn the data more effectively.

2) *Model*: We compared the performance of the four models (KNN, RF, GB, and EEGNet) in the beta band for classifying UWS and MCS. Specifically, when only the beta PSD was used, there was no significant statistical difference when the four models were used (F -value = 1.141, p -value = 0.345). However, when PSD and CSP were used together in the beta band, there was a significant difference in performance when the four models (KNN, RF, GB, and EEGNet) were used

TABLE III
STATISTICAL RESULTS BASED ON PERFORMANCE BY FEATURE

| Model | KNN | | RF | | GB | | EEGNet | |
|-----------|-----------------|-----------------|-----------------|-----------------|-----------------|-----------------|-----------------|-----------------|
| Frequency | <i>t</i> -value | <i>p</i> -value | <i>t</i> -value | <i>p</i> -value | <i>t</i> -value | <i>p</i> -value | <i>t</i> -value | <i>p</i> -value |
| Delta | -6.670 | <0.001 | -4.266 | <0.001 | -4.208 | <0.001 | -1.606 | 0.125 |
| Theta | -9.386 | <0.001 | -9.463 | <0.001 | -9.933 | <0.001 | -4.527 | <0.001 |
| Alpha | -7.044 | <0.001 | -7.229 | <0.001 | -8.037 | <0.001 | -8.769 | <0.001 |
| Beta | -2.185 | 0.042 | -2.123 | 0.048 | -2.311 | 0.038 | -2.115 | 0.048 |
| Gamma | -5.904 | <0.001 | -5.523 | <0.001 | -5.644 | <0.001 | -4.449 | <0.001 |

(F -value = 5.384, p -value = 0.003). In the post hoc test, there was a statistically significant difference only between the cases of EEGNet and GB and the cases of GB and KNN. In some cases, other models performed better than EEGNet in non-beta bands, but EEGNet performed the best in the beta band. In most cases, the superior performance of EEGNet is believed to be due to the fact that deep learning includes a process of extracting meaningful features.

3) *Frequency Band*: When comparing performances according to five frequencies, statistical validity was verified only when EEGNet was used. When PSD was used, all five performances showed significant differences (F -value = 86.344, p -value < 0.001), and in the post hoc test, there were statistical differences in all cases except when comparing the delta and theta bands. Also, when PSD and CSP were used together, there was a statistical difference in the classification performance according to the five frequencies (F -value = 72.560, p -value < 0.001). In the post-hoc test, there was no difference in the t -test results of alpha and gamma bands, beta and gamma bands, and all other results had statistically significant differences. Specifically, the performance using the beta band was high.

In DoC studies, differences between MCS and UWS were mostly revealed in the delta and alpha bands, but were rarely evident in higher frequencies such as the beta band [29]. However, low beta (12–17.75 Hz) power in MCS was significantly higher compared with UWS [30]. Also, from the perspective of the pharmacological state of consciousness, global and local efficiency in the beta band was observed to increase only when consciousness disappears and emerges during propofol-induced sedation [13]. It seems to reflect the connection between hypersynchrony and the transition to consciousness [31]. Ultimately, the increased beta power may entail a significant delay in the feedback processing of the corticothalamic network, which may lead to a network reset in which a new state configuration is obtained [13]. Therefore, in DoC patients, MCS and UWS are considered to be distinct features, given the distinct differences in feedback in the beta band, which in turn leads to increased classification performance.

B. EEG Spatial Patterns According to Awareness

We examined the CSP to identify key brain regions that differ significantly between MCS and UWS. CSP is effective in capturing the most distinctive differences between the two groups (i.e., UWS and MCS), as shown in Fig. 1. We compared CSPs, especially when using the beta band and EEGNet,

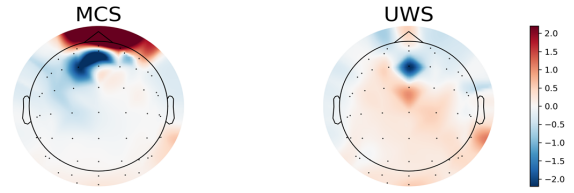


Fig. 1. CSP for classifying UWS and MCS in the beta band. The left and right represent MCS and UWS, respectively. Red regions indicate positive values and blue regions indicate negative values.

where the highest performance was observed. MCS and UWS showed large differences in variance mainly in the parietal-occipital region, which is consistent with the posterior hot zone. This is known to be directly related to the neural correlates of consciousness [13], [20]. These contributions to the level of consciousness highlight the importance of the posterior cortex in human consciousness, suggesting that this region may not only be a hub for the default mode network but also play a critical role in the subcortical integration of arousal and awareness in human consciousness [32].

C. Limitations

This study has several limitations. First, the small dataset size may have restricted the model's ability to generalize, potentially limiting its applicability across various environments. We focused on the classification of UWS and MCS, but there is a need to further refine the classification criteria, such as MCS+ or MCS-. Additionally, the diagnosis was only based on behavioral assessments and thus it is possible that some UWS were cognitive motor dissociation. Future research should aim to improve the reliability and generalization of the models by utilizing larger datasets. In addition, in order to improve generalization ability, this study evaluated with 10-fold cross-validation to identify important features and models, but an approach such as leave-one-subject-out cross-validation is needed in future studies. Second, this study focused exclusively on resting-state EEG data, and further validation is required to evaluate its performance on task-based EEG data. Additionally, exploring various feature extraction techniques and model architectures could help further elucidate the differences between MCS and UWS. Such studies would ultimately contribute to more accurate diagnoses and improved treatment strategies for DoC patients. Finally, there are quite a few reports that brain activity in other frequency regions, such as the alpha band rather than the beta band, is related to consciousness. Therefore, a procedure is needed to interpret our results through deep learning by introducing explainable artificial intelligence techniques.

IV. CONCLUSION

In this study, we performed binary classification using resting-state EEG signals of DoC patients using four models to distinguish UWS and MCS patients. We focused on the spatial features related to consciousness and demonstrated that the classification performance was higher when PSD and CSP

were used together. Next, when each of the five frequencies was used, we confirmed that the beta band, which showed a prominent difference in local efficiency in terms of the brain network, greatly improved the classification performance. In addition, among the four models, EEGNet, which was optimized for EEG signals rather than existing machine learning models, showed the best performance.

Future studies should focus on collecting larger datasets to enhance model robustness and generalizability. In addition, developing novel deep learning models tailored specifically for DoC patient classification could further optimize performance. Exploring other neurophysiological biomarkers and integrating advanced signal processing may also contribute to more precise diagnostic tools.

REFERENCES

- [1] M. Lee and S. Laureys, "Artificial intelligence and machine learning in disorders of consciousness," *Curr. Opin. Neurol.*, pp. 10–1097.
- [2] S. Chennu, L. O'Connor, R. Adapa, D. K. Menon, H. Cassol, R. Marotta, B. Kimm, Y. Zhang, and et al., "Brain networks predict metabolism, diagnosis and prognosis at the bedside in disorders of consciousness," *Brain*, vol. 140, no. 8, pp. 2120–2132, 2017.
- [3] J. L. Bernat, "Chronic disorders of consciousness," *Lancet*, vol. 367, no. 9517, pp. 1181–1192, 2006.
- [4] M. Amiri, P. M. Fisher, F. Raimondo, A. Sidaros, M. Cacic Hribljan, M. H. Othman, I. Zibrandtsen, S. S. Albrechtsen, O. Bergdal, A. E. Hansen et al., "Multimodal prediction of residual consciousness in the intensive care unit: the CONNECT-ME study," *Brain*, vol. 146, no. 1, pp. 50–64, 2023.
- [5] J. Kalafatovich, M. Lee, and S.-W. Lee, "Decoding declarative memory process for predicting memory retrieval based on source localization," *PLoS One*, vol. 17, no. 9, p. e0274101, 2022.
- [6] S. Ballanti, S. Campagnini, P. Liuzzi, B. Hakiki, M. Scarpino, C. Macchi, C. M. Oddo, M. C. Carrozza, A. Grippo, and A. Mannini, "EEG-based methods for recovery prognosis of patients with disorders of consciousness: a systematic review," *Clin. Neurophysiol.*, vol. 144, pp. 98–114, 2022.
- [7] S. Chennu, P. Finoia, E. Kamau, J. Allanson, G. B. Williams, M. M. Monti, V. Noreika, A. Arnatkeviciute, A. Canales-Johnson, F. Olivares et al., "Spectral signatures of reorganised brain networks in disorders of consciousness," *PLoS Comput. Biol.*, vol. 10, no. 10, p. e1003887, 2014.
- [8] L. Wang, W. Wang, T. Yan, J. Song, W. Yang, B. Wang, R. Go, Q. Huang, and J. Wu, "Beta-band functional connectivity influences audiovisual integration in older age: an EEG study," *Front. Aging Neurosci.*, vol. 9, p. 239, 2017.
- [9] C. Herrmann and T. Demiralp, "Human eeg gamma oscillations in neuropsychiatric disorders," *Clin Neurophysiol.*, vol. 116, no. 12, pp. 2719–2733, 2005.
- [10] D. Lehmann, P. Faber, P. Achermann, D. Jeanmonod, L. R. Gianotti, and D. Pizzagalli, "Brain sources of EEG gamma frequency during volitionally meditation-induced, altered states of consciousness, and experience of the self," *Psychiatry Res. Neuroimaging*, vol. 108, no. 2, pp. 111–121, 2001.
- [11] S. Raveendran, R. Kanchaiah, S. Kumar, J. Sahoo, M. Farsana, R. Chowdary Mundlamuri, S. Bansal, V. Binu, A. Ramakrishnan, S. Ramakrishnan et al., "Variational mode decomposition-based EEG analysis for the classification of disorders of consciousness," *Front. Neurosci.*, vol. 18, p. 1340528, 2024.
- [12] C. Porcaro, M. Marino, S. Carozzo, M. Russo, M. Ursino, V. Ruggiero, C. Ragno, S. Proto, and P. Tonin, "Fractal dimension feature as a signature of severity in disorders of consciousness: an EEG study," *Int. J. Neural Syst.*, vol. 32, no. 07, p. 2250031, 2022.
- [13] M. Lee, R. D. Sanders, S.-K. Yeom, D.-O. Won, K.-S. Seo, H. J. Kim, G. Tononi, and S.-W. Lee, "Network properties in transitions of consciousness during propofol-induced sedation," *Sci. Rep.*, vol. 7, no. 1, pp. 1–13, 2017.
- [14] M. Lee, J.-H. Jeong, Y.-H. Kim, and S.-W. Lee, "Decoding finger tapping with the affected hand in chronic stroke patients during motor imagery and execution," *IEEE Trans. Neural Syst. Rehabil. Eng.*, vol. 29, pp. 1099–1109, 2021.
- [15] M. Lee, H.-Y. Park, W. Park, K.-T. Kim, Y.-H. Kim, and J.-H. Jeong, "Multi-task Heterogeneous Ensemble Learning-based Cross-Subject EEG Classification under Stroke Patients," *IEEE Trans. Neural Syst. Rehabil. Eng.*, 2024.
- [16] V. J. Lawhern, A. J. Solon, N. R. Waytowich, S. M. Gordon, C. P. Hung, and B. J. Lance, "EEGNet: a compact convolutional neural network for EEG-based brain-computer interfaces," *J. Neural Eng.*, vol. 15, no. 5, p. 056013, 2018.
- [17] O. Bodart, O. Gosseries, S. Wannez, A. Thibaut, J. Annen, M. Boly, M. Rosanova, A. G. Casali, S. Casarotto, G. Tononi et al., "Measures of metabolism and complexity in the brain of patients with disorders of consciousness," *NeuroImage: Clinical*, vol. 14, pp. 354–362, 2017.
- [18] O. Bodart, E. Amico, F. Gómez, A. G. Casali, S. Wannez, L. Heine, A. Thibaut, J. Annen, M. Boly, S. Casarotto et al., "Global structural integrity and effective connectivity in patients with disorders of consciousness," *Brain Stimul.*, vol. 11, no. 2, pp. 358–365, 2018.
- [19] M. Rosanova, M. Fecchio, S. Casarotto, S. Sarasso, A. G. Casali, A. Pigorini, A. Comanducci, F. Seregini, G. Devalle, G. Citerio et al., "Sleep-like cortical OFF-periods disrupt causality and complexity in the brain of unresponsive wakefulness syndrome patients," *Nat. Commun.*, vol. 9, no. 1, p. 4427, 2018.
- [20] M. Lee, L. R. Sanz, A. Barra, A. Wolff, J. O. Nieminen, M. Boly, M. Rosanova, S. Casarotto, O. Bodart, J. Annen et al., "Quantifying arousal and awareness in altered states of consciousness using interpretable deep learning," *Nat. Commun.*, vol. 13, no. 1, p. 1064, 2022.
- [21] M. J. Hasan, D. Shon, K. Im, H.-K. Choi, D.-S. Yoo, and J.-M. Kim, "Sleep state classification using power spectral density and residual neural network with multichannel EEG signals," *Appl. Sci.*, vol. 10, no. 21, p. 7639, 2020.
- [22] C. C. W. Fadzal, W. Mansor, L. Y. Khuan, N. B. Mohamad, Z. Mahmoodin, S. Mohamad, and S. Amirin, "Welch power spectral density of eeg signal generated from dyslexic children," *2014 IEEE Reg. 10 Symp.*, pp. 560–562, April 2014.
- [23] K. Darvish Ghanbar, T. Yousefi Rezaii, A. Farzamnia, and I. Saad, "Correlation-based common spatial pattern (CCSP): A novel extension of CSP for classification of motor imagery signal," *PLoS One*, vol. 16, no. 3, p. e0248511, 2021.
- [24] M. Ala'raj, M. Majdalawieh, and M. F. Abbod, "Improving binary classification using filtering based on k -NN proximity graphs," *J. Big Data*, vol. 7, no. 1, p. 15, 2020.
- [25] A. J. Ferreira and M. A. Figueiredo, "Boosting algorithms: A review of methods, theory, and applications," *Ensemble Mach. Learn.*, pp. 35–85, 2012.
- [26] P. Liuzzi, A. Magliacano, F. De Bellis, A. Mannini, and A. Estraneo, "Predicting outcome of patients with prolonged disorders of consciousness using machine learning models based on medical complexity," *Sci. Rep.*, vol. 12, no. 1, p. 13471, 2022.
- [27] M. Lee, H. Kang, S.-H. Yu, H. Cho, J. Oh, G. Van Der Lande, O. Gosseries, and J.-H. Jeong, "Automatic Sleep stage Classification Using Nasal Pressure Decoding Based on a Multi-Kernel Convolutional BiLSTM Network," *IEEE Trans. Neural Syst. Rehabil. Eng.*, 2024.
- [28] M. Sokolova, N. Japkowicz, and S. Szpakowicz, "Beyond accuracy, F-score and ROC: a family of discriminant measures for performance evaluation," *Australas. Jt. Conf. Artif. Intell.*, pp. 1015–1021, 2006.
- [29] Y. Bai, Y. Lin, and U. Ziemann, "Managing disorders of consciousness: the role of electroencephalography," *J. Neurol.*, vol. 268, pp. 4033–4065, 2021.
- [30] A. Piarulli, M. Bergamasco, A. Thibaut, V. Cologan, O. Gosseries, and S. Laureys, "EEG ultradian rhythmicity differences in disorders of consciousness during wakefulness," *J. Neurol.*, vol. 263, pp. 1746–1760, 2016.
- [31] K. Kuizenga, J. Wierda, and C. Kalkman, "Biphasic EEG changes in relation to loss of consciousness during induction with thiopental, propofol, etomidate, midazolam or sevoflurane," *Br. J. Anaesth.*, vol. 86, no. 3, pp. 354–360, 2001.
- [32] B. L. Edlow, "Dopaminergic modulation of human consciousness via default mode network connectivity," *Proc. Natl. Acad. Sci. U.S.A.*, vol. 118, no. 31, p. e2111268118, 2021.